Development of a Novel Probe for Measuring Drug Binding to the *F1*S* Variant of Human Alpha 1-Acid Glycoprotein

LAWRENCE P. COGSWELL III,[1,2] DOUGLAS E. RAINES,[3] SONALI PAREKH,[4] OLIVER JONAS,[1] JOHN E. MAGGIO,[5] GARY R. STRICHARTZ[1,2,6]

[1]Pain Research Center, Department of Anesthesiology, Perioperative and Pain Medicine, Brigham & Women's Hospital, 75 Francis Street, Boston, Massachusetts 02115

[2]Harvard Biophysics Program, Harvard University, Boston, Massachusetts

[3]Department of Anesthesia and Critical Care Medicine, Massachusetts General Hospital, Boston, Massachusetts

[4]Brown University School of Medicine, Providence, Rhode Island

[5]Department of Pharmacology and Cell Biophysics, University of Cincinnati College of Medicine, Cincinnati, Ohio

[6]Department of Biological Chemistry and Molecular Pharmacology, Harvard Medical School, Boston, Massachusetts

Received 31 May 2000; revised 20 February 2001; accepted 5 March 2001

ABSTRACT: A novel probe was developed to measure drug association with the *F1*S* variant of the human serum protein alpha 1-acid glycoprotein (AGP). The molecule 2-hydroxy-3,5-diiodo-*N*-[2(diethylamino)ethyl]benzamide (DEDIC) binds to AGP, quenching its native fluorescence. This quenching was fitted to a two-site model giving apparent dissociation constants of 0.049 ± 0.005 and 12 ± 2 μM (mean ± SEM). Quenching of each of the separate variants of AGP by DEDIC was itself described by a two-site model, giving for the *F1*S* variant $K^1_{D(F1*S)} = 0.041 \pm 0.010$ μM and $K^2_{D(F1*S)} = 29 \pm 7$ μM; and for the *A* variant $K^1_{D(A)} = 0.31 \pm 0.18$ μM and $K^2_{D(A)} = 8.8 \pm 0.7$ μM. The utility of DEDIC in probing drug interactions with isolated variants was demonstrated in competition experiments with the model drugs amitriptyline and bupivacaine. In addition, the selectivity of DEDIC for variant *F1*S* rendered it capable of probing the binding of drugs (including the variant *A*-selective drug amitriptyline) to *F1*S* in a mixture of variants, such as occurs naturally in whole AGP. DEDIC is unique as an *F1*S* variant-selective probe of drug binding to whole AGP that is also sufficiently soluble to serve as a probe of drug binding to the lower affinity sites on isolated *A* and *F1*S* variants. J Pharm Sci 90:1407–1423, 2001

Keywords: alpha 1-acid glycoprotein; drug binding; genetic variants; probes; methods

INTRODUCTION

Characterizing the association of blood-borne drugs with the major serum protein alpha 1-acid glycoprotein (AGP) is a problem of general pharmacological interest. Many drugs are bound, principally or in part, by AGP,[1] and AGP is the principal carrier of basic drugs in plasma.[2,3] The extent of this association, at equilibrium, determines the concentration of unbound drug, and the traditional thought is that only this fraction is available for active uptake or diffusion into surrounding tissues. Clinically, this buffering effect must be considered in adjusting the dosage

Correspondence to: G. R. Strichartz (Telephone: 617-732-8797; Fax: 617-730-2801)

Journal of Pharmaceutical Sciences, Vol. 90, 1407–1423 (2001)

of a drug or in assessing the toxicity of a drug accidentally administered intravenously, a feat that is often complicated by changes in patients' AGP concentrations during disease, pregnancy, or other conditions.[2]

The heterogeneity of AGP adds an additional level of complexity. There are three major variants of AGP (*F1*, *S*, and *A*), which differ from one another in primary structure[4] and which may be separated after desialylation using polyacrylamide gel isoelectric focusing.[5] This heterogeneity is important to consider when carrying out binding studies with AGP, because the *A* variant has been reported to bind many drugs with affinities different from those of the *F1* or *S* variant.[1,6,7]

The genetic polymorphism is the result of the existence of two different genes that encode for AGP.[8] One of these, denoted *AGP-A*, encodes the *F1* and *S* variants, whereas the other, *AGP-B*/*B'*, encodes the *A* variant.[9] The relative frequency of the major phenotypes is ~50% *F1*S*/*A*, 35% *F1*/*A*, and 15% *S*/*A*, and the relative abundance in commercial, pooled-source protein of the *F1*, *S*, and *A* variants has been reported to be 44 ± 1, 29 ± 1, $27 \pm 1\%$, respectively.[7] Structurally, the two genes differ by 22 codons, resulting in 22 amino acid substitutions along the protein of 183 residues. The *F1* and *S* variants, conversely, are reported to differ from each other by fewer than five residues.[8] In addition to the *F1*, *S*, and *A* variants, there exist a multitude of minor gene products that arise from the multiple allelic forms of AGP-*A* and AGP-*B*/*B'*.[4] However, these products, in total, account for $< 1\%$ of the AGP encountered in the general population[6] and are not likely to be significant sources of drug binding.

Because drugs have been observed to bind differently to the *A* variant than to the *F1* or *S* variants (collectively denoted *F1*S*),[1,6,7] it is clear that understanding the pharmacological role of AGP will require an examination of how drugs interact with each of these variants individually.[1] Furthermore, a complete characterization must include a determination of affinities for both the higher and lower affinity sites on each.

Commercially available AGP is derived from pooled human plasma, and consists of ~70% *F1*S* and 30% *A* variants,[5,6,7] reflecting the population average. To accurately determine binding affinities, these variants must first be separated, for example, according to the chromatographic methods described by Hervé[10] and Halsall.[11] Indeed, the failure to do so may account for some of the inconsistent results and fractional binding site stoichiometries obtained over the years in drug binding studies with AGP.

We have developed a rapid spectrofluorometric method for determining drug affinities to the high affinity site on the *F1*S* variant of AGP in a heterogeneous mixture using the novel molecule 2-hydroxy-3,5-diiodo-*N*[2(diethylamino)ethyl] benzamide (DEDIC). The method is based on spectrofluorometry, which has considerable advantages over equilibrium dialysis in terms of speed, convenience, and sensitivity.[12]

In short, DEDIC binds to and quenches the native tryptophan fluorescence of AGP. Subsequent addition of a nonquenching drug that is known to bind AGP, such as bupivacaine (BUP) or amitriptyline (AMI), results in fluorescence recovery from which the binding constant of the antagonist may be calculated.

In addition, we demonstrate that DEDIC binds selectively to the high affinity site on the *F1*S* variant of AGP and can be used to probe the association of a drug to this site in the naturally occurring mixture of the two proteins. The selectivity of DEDIC for a single site on one of the AGP variants, coupled with a solubility sufficient to permit its use as a probe of drug binding to lower affinity sites on (isolated) single variants, distinguishes it from other (fluorescent) probes currently in use (e.g., 8-anilinonapthalensulfonic acid, ANS). Among quenchers, DEDIC possesses a significant advantage over other potentially useful probes. Chlorpromazine (CPZ), for example, is not variant selective, whereas dipyridamole (DIP) is variant selective to the same extent as DEDIC (~10-fold) but not sufficiently soluble that it can be used on isolated variants to probe lower affinity binding.

EXPERIMENTAL PROCEDURES

Caution

The following chemicals are hazardous and should be handled carefully: *N, N*-diethylethylenediamine, thionyl chloride, and 1,4-dioxane.

Materials

Human alpha 1-acid glycoprotein (AGP, lot 125H9329), dipyridamole (DIP), amitriptyline (AMI), and bupivacaine (BUP), all $> 99\%$ pure,

were obtained from Sigma Chemical Company (St. Louis, MO). *N,N*-Diethylethylenediamine (DED, 99%), 3,5-diiodosalicylic acid (DIS, 99%), 1,4-dioxane (99.8%, anhydrous), thionyl chloride ($SOCl_2$, 97%), and diethyl ether (99 + %, anhydrous) were obtained from Aldrich Chemical Company (Milwaukee, WI). Ethanol (EtOH, 100%, anhydrous) in glass bottles was obtained from Pharmco Products (Brookfield, CT). All other chemicals were ACS reagent grade obtained from Aldrich. Water was doubly deionized to > 18.2 MΩ with a Milli-Q ultra pure water system (Millipore Corp., Woburn, MA) and was free of fluorescent contaminants. Iminodiacetic acid (immobilized on Sepharose 6B Fast Flow Gel) and copper(II) chloride were obtained from Sigma.

Synthesis of DEDIC

First, 30 g (0.077 mol) of DIS were added to 120 mL of $SOCl_2$ and the suspension was refluxed under dry nitrogen at 120°C for 40 min. $SOCl_2$ was evaporated at 130°C over a steady nitrogen stream until a clear, light yellow oil remained. Remaining $SOCl_2$ was evaporated at 2 Torr for 2 min, yielding a viscous yellow-brown oil. This residue solidified on cooling to 20°C *in vacuo*. The residue was removed from vacuum and dissolved in 150 mL of dioxane, heating as necessary, to give a clear, light yellow solution. Aliquots (3 mL) of this solution were added at 1-min intervals to 50 g (0.44 mol) neat DED with gentle stirring. A voluminous yellow precipitate formed in the recipient flask before addition was complete, and several milliliters of additional dioxane were added to facilitate stirring. After standing for 1 h at 20°C, the mixture was vacuum filtered, and the resinous yellow solid was washed thrice with 25 mL of 1.0 M HCl to remove excess amine salts. The solid was then agitated with a spatula and washed liberally with deionized water until a powdery solid remained. The product was washed four times with 10 mL of ethanol and three times with 25 mL of ether, and allowed to dry on the funnel. Sixteen grams of crude product were recovered and then dissolved in a minimum (~100 mL) of boiling methanol. This solution was gravity filtered and then decanted into a crystallizing dish at room temperature. After 24 h at 20°C, white crystals were collected on a glass frit and washed with a minimum of cold methanol and then with 5 mL ether. The product was dried overnight in a vacuum oven at 20 Torr and 70°C. The yield was 8.0 g (0.017 mol; 22%).

Structure Determination

Nuclear magnetic resonance (NMR) measurements were performed on a Bruker 500 MHz instrument at 20°C in either deuterated chloroform or a 1:2 v/v mixture of deuterated water and methanol. Isotopic purity for all solvents was $> 99.9\%$. pH was adjusted with sodium deuteroxide or deuterium chloride from 2 to 13, as measured by spotting a drop of solution onto pHydrion-brand pH paper (Microessential Laboratories, Brooklyn, NY). The precision of the paper is ± 0.5 pH unit. Low-resolution fast atom bombardment mass spectroscopy (FABMS) was performed in a glycerol matrix in the positive ion mode.

Elemental Analysis

Standard C, H, N analysis was performed, as well as I and Cl analysis, using ion-selective electrodes.

Chemical Stability

Aqueous DEDIC solutions at pH 3, 7.4, and 12 were stored at either room temperature (19–20°C)/room light, room temperature/dark, or 4°C/dark. Hydrolysis was measured as free DIS, and photo-deiodination as aqueous iodine, which were easily detected spectrophotometrically.

Preparation of Biochemical Solutions

Except where noted, all solutions were prepared in standard aqueous medium (SAM), containing 0.15 M NaCl and 5 mM MOPS buffer adjusted to pH 7.40. Glassware was triply rinsed with double-deionized water and oven dried prior to use. For fluorescence experiments, glassware was initially cleaned with 7 M HNO_3 to degrade any adsorbed fluorescent contaminants; plastic containers were avoided. Determinations of mass were made on a Mettler AE100 electronic balance and were accurate to ± 0.0002 g as determined with standard weights. Adjustable volumetric pipettes (Gibson or Eppendorf) were used routinely and fitted with polypropylene tips that were observed not to contaminate solutions with fluorescent plasticizers. Solutions were covered with aluminum foil, Teflon tape, or glass stoppers (no grease).

Solutions of whole AGP were prepared gravimetrically, using a molecular weight of

40,800 g/mol and water content of 13% (Sigma Chemical Co., personal communication). The molar absorptivity of whole AGP was determined to be 3.24×10^4 $M^{-1}cm^{-1}$, and this value was used to determine the concentration of the isolated *F1*S* and *A* variants. In so doing, we assumed that absorbance by the tryptophan chromophores was unaffected by the substitution of other residues. This assumption is supported by the observation that scaled absorbance spectra of AGP, *F1*S*, and *A* variant are identical (data not shown), a situation that could arise in practice only if amino acid substitution did not affect the chromophores.

DEDIC solutions were prepared by adding the solid material to SAM and stirring vigorously to form a suspension. Aqueous HCl (1 M) was then added in a dropwise manner until the solid dissolved. The pH of the solution was immediately readjusted to pH 7.40 with NaOH. Ultraviolet–visible (UV–vis) spectroscopy confirmed that DEDIC was not hydrolyzed by this procedure. DEDIC was soluble in SAM at pH 7.40 to ~250 μM. Although it is possible to form nominally more concentrated solutions, in our experience these are, in fact, supersaturated, and slow aggregation may occur over a period of hours to days.

DIP solutions were similarly prepared by initial acidification to speed dissolution. The solubility limit was ~5 μM in SAM.

Optical Titration

Spectrophotometric titrations were performed at 22°C with a Beckman DUS model 600 single-beam spectrophotometer with matched far UV quartz cuvettes. Spectrofluorometric titration was performed with an Aminco SPF 500 spectrofluorometer. The pK_as were determined either by plotting the observed λ_{max} versus pH or by first computing the ratio of absorbances (fluorescences) at two wavelengths corresponding to the λ_{max}s for the conjugate acid and base, and then plotting versus pH. pH was measured with a Corning combination electrode with an Orion digital pH meter (model 611).

Fluorescence Assays

Emission scans were performed in ratio mode at 22°C with an SLM-Aminco SPF-500 spectrofluorometer using rhodamine B (3 g/L in ethylene glycol) as reference. Slits were 7.5 nm, and the excitation wavelength was 278 nm, except as noted. The emission spectrum of AGP was essentially independent of excitation wavelength over the range 265–295 nm (data not shown), indicating that tyrosine residues did not contribute significantly to the observed fluorescence. Therefore, the protein was excited at its wavelength of maximum absorbance (278 nm) to give maximal fluorescence. Quartz cuvettes were soaked daily in 7 N HNO_3 for 30 min. Cuvettes were fitted with copper handles and not touched with gloves or paper tissues. Between scans, cuvettes were cleaned with ethanol dispensed from glass bottles and dried over air filtered through a 0.2-μM filter (Gelman PTFE ACRODisk).

Analysis of Steady-State Fluorescence Data

Raw fluorescence data (F_{raw}) were first corrected for inner filter effects[13] and second for spurious fluorescence (e.g., from Raman scatter.) Third, data were corrected for the fluorescence contribution of the drug, if any. For ligands used in this study, this correction was minimal and accounted for $< 10\%$ of the total signal. The corrected fluorescence, normalized to unity (F), was then plotted versus nominal [DEDIC] and fitted directly to modified Stern–Volmer equations allowing for either one (eq. 13) or two (eq. 26) classes of binding sites either on the same or different protein molecules (see Appendix). The derivations of these equations is complicated by the inapplicability of common simplifying assumptions in our experiments. Most significantly, because our ligand concentrations were comparable to those of the protein, we were unable to approximate the concentration of free ligand at equilibrium by its nominal (total) concentration. Equations 13 and 26 (Appendix) are, therefore, exact descriptions of the isotherms.

In some experiments, a titration method was used instead, wherein successive aliquots of drug were added *in situ* to a cuvette containing 2.5 mL of protein solution. To minimize the possibility of degradation associated with repeated interrogation of the sample, single wavelength measurements ($\lambda_{em} = 345$ nm) were collected instead of complete emission scans, and the excitation shutter was closed between measurements. Fluorescence data were first corrected for inner-filter effects[13] and then corrected for dilution by multiplying each datum by the appropriate dilution factor. Under the conditions used in this study

(where the concentration of stock titrant exceeded the K_D or K_I by a factor of at least 50), the effect of volume dilution on the free fraction of protein was assumed to be negligible. This assumption was confirmed for quenching by DEDIC both theoretically by simulations conducted using Mathematica® software (Wolfram Research) and experimentally by direct comparison of data collected using both the titration method and the method of individual aliquots.

Assessing the Significance of Dynamic Quenching

The contribution of dynamic quenching was deemed to be negligible for the concentrations of protein and quencher used in this study (i.e., [AGP] < 5 μM, and [Drug] < 50 μM) according to the following argument. Assuming a maximum, diffusion-limited, collision rate of drug and protein equal to 10^{10} M^{-1} s^{-1}, and a quencher concentration of 5×10^{-5} M, the rate of collision of quencher with AGP is 5×10^5 s^{-1}. The average time between collisions on any given AGP molecule is thus ~2 μs. The fluorescence lifetimes of the tryptophans in AGP have been reported to be on the order of 1–10 ns,[14] which is 200–2000 less than the average time between collisions, effectively obviating a role for dynamic quenching.

Chromatographic Separation of Variants

AGP was separated chromatographically into the major variants *F1*S* and *A* using Halsall's modification[15] of Hervé's method.[10] Briefly, a 20-cm column (i.d. = 1 cm) containing ~40 mL of iminodiacetic acid (immobilized on Sepharose 6B Fast Flow Gel) was allowed to equilibrate with several volumes of 0.2 M copper(II) chloride/150 mM NaCl and then rinsed with several volumes of pH 3.8 100 mM acetic acid/150 mM NaCl, followed by several volumes of the standard pH 7 buffer, SAM (150 mM NaCl/5 mM MOPS). Whole AGP, 25 mg in 1 mL SAM, was applied to the column and eluted at a constant flow rate of 6 mL/min. Elution was monitored spectrophotometrically by scanning over the wavelength range 210 to 450 nm, and fractions of 5 to 20 mL each were collected. After elution of the adsorbing component (*F1*S*), the pH of the elution buffer was stepped down to 4.6 to elute the *A* variant. The column was reconditioned between runs by removing chelated copper with 50 mM EDTA, pH 7, rinsing with several volumes of deionized water, and repeating the equilibration procedure. The relative yield of each component was determined using absorbance data at 280 nm and our previously determined molar absorptivity for whole AGP of 3.24×10^4 M^{-1} cm^{-1}. Fractions from the *F1*S* and *A* variant components were pooled separately. Because they were eluted in the same buffer to be used in subsequent fluorescence measurements and the concentration of each variant (as determined spectrophotometrically) was sufficiently large, concentration and dialysis steps were unnecessary.

Confirmation of the Identity of the Variants

The identification of the separated variants was made by comparing our relative yield of each variant with that reported by Halsall.[15] In addition, the *F1*S* variant-selective drug DIP was added to equal concentrations (0.39 μM) of *F1*S* variant, *A* variant, and whole AGP. From the resulting quench curves, the affinity of DIP for each variant was determined. The relative affinities of the drugs were compared with those previously reported using a different method and different (phosphate) buffer.[1]

Competition between DEDIC and AMI on Whole AGP and Its Isolated Variants

The model drug AMI was added to partially quenched solutions of DEDIC and protein. From the resulting fluorescence recovery curves, the affinities of these drugs were determined by fitting the data to a model of competitive antagonism at a single site (see Appendix, eq. 36) The concentration of DEDIC was chosen so that only a single high affinity site would be occupied and competition at lower affinity sites was negligible. Where experiments were repeated at several [DEDIC], the data were fit simultaneously to eq. 36.

RESULTS

Structure of DEDIC

The consensus structure of the novel molecule DEDIC is shown in Figure 1A. From the ^1H NMR spectra in 2:1 v/v CD_3OD/D_2O (Figure 1B), peak assignments were made as reported in Table I. No impurities were detected. Low-resolution FABSMS gave an M+1 ion peak at $m/z = 489$ consistent with the calculated molar mass of DEDIC of 488 g/mol.

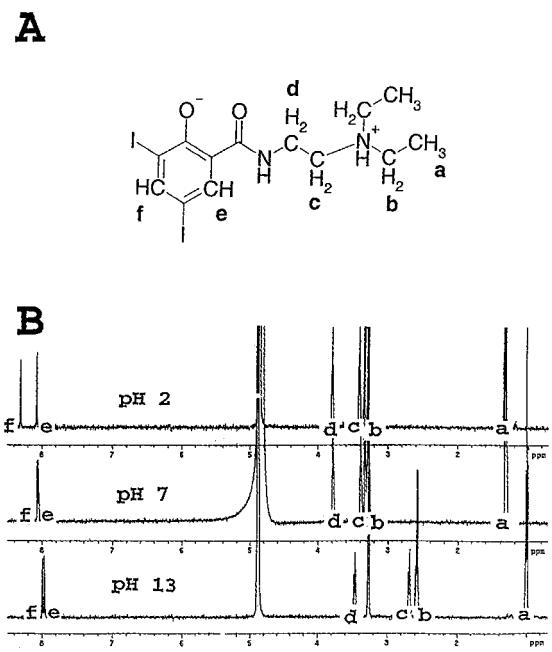

Figure 1. (**A**) Structure of the novel molecule DEDIC. Chemically distinct hydrogen nuclei are identified by bold letters. (**B**) ^{1}H NMR spectra of DEDIC (in 2:1 v/v D_2O/CD_3OD, room temperature) at pH 2 (top) , pH 7 (middle) and pH 13 (bottom). (See Figure 1 for an assignment of resonances.) From pH 2 to pH 7 (top to middle traces) the aromatic resonance **f** shifts upfield as the phenol moiety of DEDIC is deprotonated, and from pH 7 to pH 13 (middle to bottom traces) the resonances of the aliphatic protons (**a**–**d**) shift upfield in response to deprotonation of the tertiary amine. Isotopic impurities in the solvents cause the strong resonances at $\delta = 3.3$ and 4.9 ppm. The internal reference was sodium-3-(trimethylsilyl)propionate-2,2,3,3-d_4.

Elemental analysis (C, H, N, I) agreed well with theory, considering the potential of phenolic compounds to form hydrates and the relatively large uncertainty in determination of iodine ($\pm 2\%$): 30.35% C (theory 31.96%), 3.84% H (theory 3.68%), 5.23% N (theory 5.73%), and 48.68% I (theory 52.0%). Furthermore, the analysis was entirely consistent with DEDIC sesquihydrate (DEDIC· 1.5 H_2O) to within $\pm 0.4\%$ for C, H, and N, and $\pm 1\%$ for I. Chloride was not detected by trace analysis (limit of detection = 0.05%), indicating that DEDIC had not crystallized as a hydrochloride salt.

Table I. Chemical Shifts[a] of Hydrogen Nuclei of DEDIC at Varying pH Values

δ (ppm) ^{1}H	pH 2	pH 7	pH 13
a	1.32	1.31	1.06
b	3.32	3.38	2.63
c	3.40	3.27	2.72
d	3.79	3.76	3.51
e	8.07	8.04	8.01
F	8.30	8.05	8.04

[a]Determined in 2:1(v/v) CD_3OD/D_2O (see Figure 1A for ^{1}H labels and 1B for raw spectra).

Physical Properties of DEDIC

The molar absorptivity of DEDIC in SAM (pH 7.40 and 22 °C) at $\lambda_{max} = 356$ nm was 5.02 (± 0.05) $\times 10^3$ $M^{-1}cm^{-1}$, determined from solutions at < 20 μM [DEDIC]. The aqueous solubility of DEDIC at pH 7.4 and room temperature was ~250 μM.

Spectrophotometric titration of DEDIC was characterized by changes in absorbance intensity and peak wavelength. Over the pH range 4–6, λ_{max} (DEDIC) shifted from 328 to 355 nm and peak absorbance rose, with an isosbestic point at 331 nm (Figure 2A, inset). pH-dependent shifts in λ_{max} as a function of pH gave $pK_a^1 = 5.0 \pm 0.2$ (Figure 2A). From pH 7 to 10, λ_{max} shifted from 355 to 351 nm, and peak absorbance remained unchanged (Figure 2B, inset). The calculated pK_a^2 of 9.5 ± 0.2 (Figure 2B) was determined by pH-dependent changes in the absorbance ratio A_{355}/A_{351} that resulted from the wavelength shift.

Because of the relatively small peak shift observed spectrophotometrically for the second protonation event, pK_a^2 was also determined by spectrofluorometric titration. The fluorescence emission spectrum of DEDIC was considerably more sensitive than absorbance to the second protonation event, as evidenced by a red shift of almost 10 nm (Figure 2C, inset). The fitted pH dependence of this shift yielded a pK_a^2 of 9.8 ± 0.2 (Figure 2C), which is consistent with that derived from absorbance changes (vide supra).

The NMR spectra in 2:1 v/v CD_3OD/D_2O (shown in Figure 1B with ^{1}H assignments provided in Table I) showed pH-dependent shifts consistent with two protonation events. On traversing pK_a^1 (i.e., increasing pH from 2 to 7), the resonance of one of the aromatic hydrogens (f) shifted significantly upfield, whereas the shifts of the aliphatic hydrogens (i.e., a–d) were relatively unaffected. Conversely, on traversing pK_a^2, the opposite response was observed, with the resonances of the aliphatic hydrogens shifting significantly upfield and those of the aromatic hydrogens remaining approximately the same.

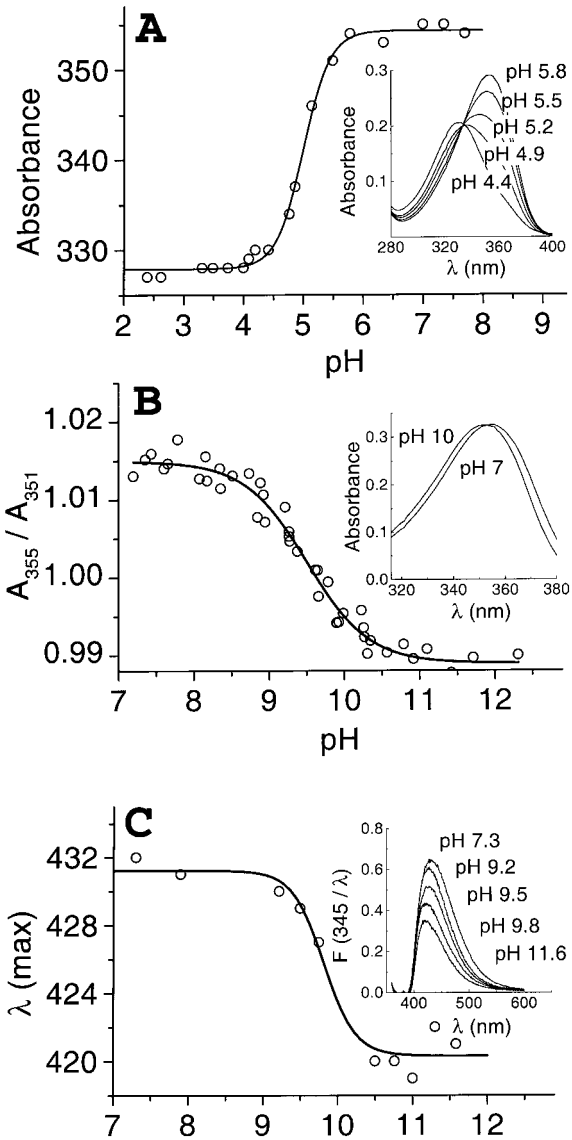

Figure 2. (**A**) Spectrophotometric titration of the acid moiety of DEDIC. λ_{max} is plotted against pH (open circles). The data were fitted to the Henderson–Hasselbalch equation (solid line), giving a pK_a^1 of 5.0 ± 0.2. Inset: λ_{max} shifts from 328 to 355 nm over the pH range 4–6, with an isosbestic point at 331 nm. (**B**) Spectrophotometric titration of the basic moiety of DEDIC. The ratio A_{355}/A_{351} (open circles) is plotted against pH. These data were fitted to the Henderson–Hasselbalch equation (solid line), giving a pK_a^2 of 9.5 ± 0.2. Inset: λ_{max} shifts bathochromically from 355 to 351 nm over the pH range 7 to 10. (**C**) Spectrofluorometric titration of the basic moiety of DEDIC. λ_{max} (open circles) is plotted against pH. These data were fitted to the Henderson–Hasselbalch equation (solid line), giving a pK_a^2 of 9.8 ± 0.2. Inset: Emission spectra of DEDIC (F 345/λ_{em}) over the pH range 7.3–11.6.

Because changes in pH around pK_a^1 resulted in shifts in the resonances of one of the aromatic protons (f) of DEDIC, this protonation event was assigned to the dissociation of hydrogen from the phenolate moiety. Likewise, the pH-dependent shifts of the aliphatic ^{1}H (a–d) resonances near pK_a^2 were attributed to protonation of the tertiary amine (see Figure 1B).

Consistent with this assignment, the optical absorbance spectrum of DEDIC changed on traversing the pH region near pK_a^1 (Figure 2A), reflecting the perturbation of the electronic structure of the aromatic ring associated with dissociation of the phenol hydrogen. Notably, DEDIC is a zwitterion at physiologic pH.

Stability

Solutions are stable in the dark for at least 1 week at 22°C and for at least 1 month at 4°C. In room light at 22°C, solutions are stable for ~2 days before traces of free iodine could be detected spectrophotometrically. DEDIC hydrolysis was negligible between pH 3 and pH 11. DEDIC was stable in the spectrofluorometer during continuous irradiation at 278 nm for at least 15 min (300 mW Hg lamp, 15 nm slit widths). Continuous excitation near the absorption maximum (356 nm) resulted in accelerated photo-deiodination, which was easily detected by yellow-brown coloration of the solution after ~15 min. The absorbance spectrum and odor of the solution were consistent with that of aqueous molecular iodine.

Separation of Protein Variants

To investigate the identities of the two apparent binding sites observed for DEDIC binding to whole protein, 25 mg of AGP was separated chromatographically into its variants (*cf.* Methods). Recovery of the protein was quantitative, with 81% of the material (as monitored spectrophotometrically) eluting in the first fraction and 19% in the second fraction (Figure 3); these proportions were similar to those reported by Halsall.[15] Furthermore, the absorbance spectra of these fractions were identical in shape to that of pure AGP. Because we had simply repeated Halsall's procedure, with changes only in the identity (MOPS rather than phosphate) and ionic strength of the eluting buffer, we therefore equated the first and second elution fraction with the *F1*S* and *A* variants, respectively, identified by Halsall.

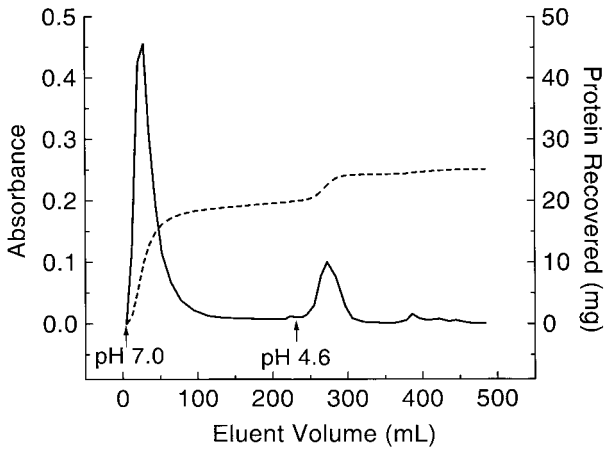

Figure 3. Chromatographic separation of AGP into the *A* and the *F1S* variant. Twenty-five milligrams of whole AGP was applied to the copper-iminodiacetate column. The absorbance at 280 nm (solid line) shows that the first fraction (*F1*S* variant) was eluted at pH 7.0 and the second fraction (*A* variant) was eluted after stepping the pH down to 4.6. The cumulative protein recovery (in milligrams) is also shown (dashed line). Total protein recovery was ~99%, with the *A* and the *F1*S* variants comprising 19 and 81%, respectively, of the material.

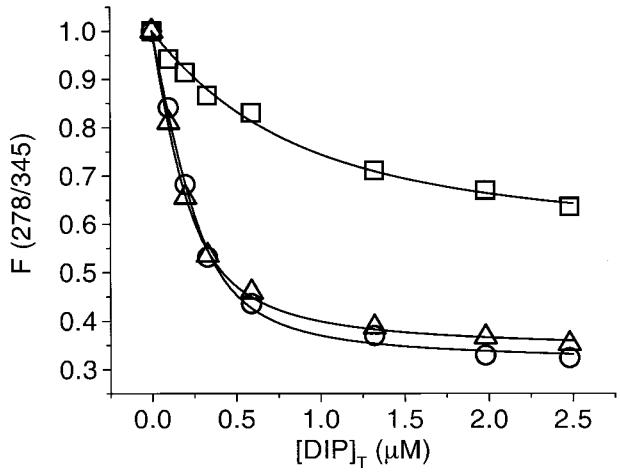

Figure 4. Fluorescence quenching of 0.39 μM AGP with added DIP. Quench data for variant *A* (squares), variant *F1S* (circles), and whole AGP (triangles) were fitted by eq. 13 to yield $K_{D(A/DIP)} = 0.75 \pm 0.12$ μM, $K_{D(F1*S/DIP)} = 0.07 \pm 0.02$ μM, and $K_{D(AGP/DIP)} = 0.84 \pm 0.14$ μM. The amplitudes of these processes were 0.48 ± 0.03, 0.69 ± 0.01, and 0.63 ± 0.01, respectively.

Confirmation of Variants Using the *F1*S*-Selective Drug DIP

Confirmation of variants was made by determining the affinities of the *F1*S* variant-selective drug DIP to the isolated variants and comparing these to previously reported values.

The DIP quench data (Figure 4) were fit by a modified one-site Stern–Volmer equation (eq. 13) to give affinities of $K_{D(A/DIP)} = 0.75 \pm 0.12$ μM and $K_{D(F1*S/DIP)} = 0.07 \pm 0.02$ μM, with an n_A of 0.73 and an indeterminate n_{F1*S}. The amplitudes of these processes were 0.48 ± 0.03 and 0.69 ± 0.01, respectively. Unfortunately, solubility limitations prevented us from investigating the binding of DIP to lower affinity sites on AGP, as were reported by Hervé.[7]

Binding of DEDIC to AGP and to the Isolated Variants

The spectral changes in fluorescence during quenching of 0.44 μM whole AGP by increasing concentrations of DEDIC are depicted in Figure 5A. The emission spectrum of AGP results principally from the three tryptophan residues of the protein, and in SAM is maximal near 340 nm. Note that the *relative* degree of quenching appears to be largely independent of emission wavelength between 325 and 400 nm (Figure 5B), so any analytical wavelength in this range would be suitable. Outside this range, the apparent wavelength dependence is difficult to interpret because it may be an artifact of a decreasing signal-to-noise ratio. By convention, we have chosen a near maximal analytical wavelength (345 nm). The emission spectra of the *F1*S* and *A* variants are identical to each other and to that of whole AGP as well (data not shown).

The fluorescence intensity (ex. 278/em. 345, corrected for inner filter effects[13]) of 0.36 μM whole AGP, variant *A*, and variant *F1*S*, is shown in Figure 6 as a function of *nominal* [DEDIC]. For whole AGP (Figure 6, triangles), the concentration dependence could not be fitted satisfactorily by a one-binding-site model (eq. 13), but was fit well by a two-site model (eq. 26), using the analysis presented in the Appendix (vide infra). From nonlinear least squares regression of these data, we obtained apparent equilibrium dissociation constants for DEDIC binding to whole AGP of $K^1_{D(native)} = 0.049 \pm 0.005$ μM, $n_1 = 0.63 \pm 0.04$ μM, and $K^2_{D(native)} = 12 \pm 2$ μM, with n_2 indeterminate. The amplitudes of the two processes were $A_1 = 0.59 \pm 0.03$ and $A_2 = 0.22 \pm 0.02$ with an unquenched fraction having $A_{unq} = 0.19 \pm 0.03$.

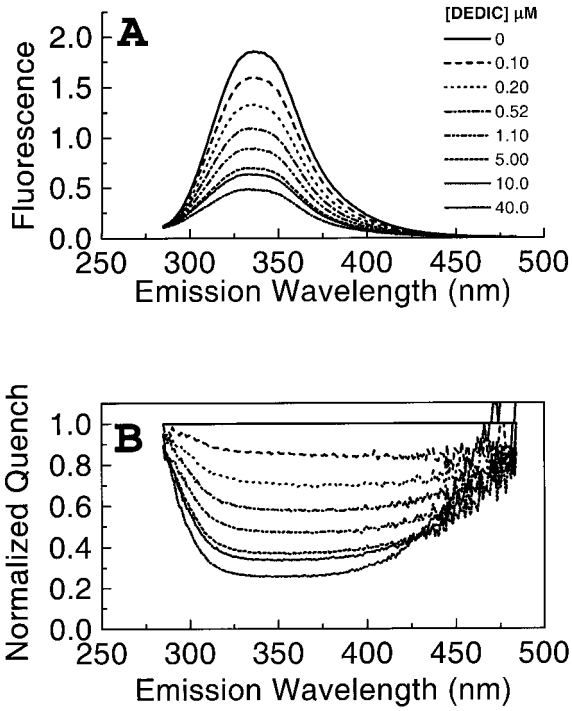

Figure 5. (**A**) Addition of increasing [DEDIC] to 0.44 μM AGP quenches the native tryptophan fluorescence of the protein. The ordinate is the corrected, normalized fluorescence (*F*) with excitation at 278 nm. Nominal [DEDIC] are as shown. (**B**) Relative quenching (defined as the quotient *F* divided by *F* in the absence of DEDIC) is invariant over a range of emission wavelengths.

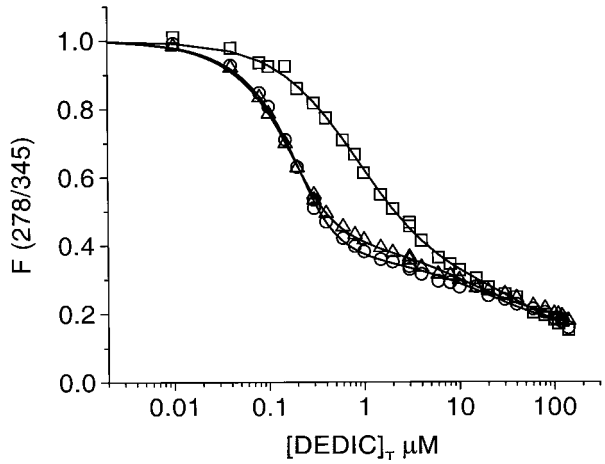

Figure 6. The corrected, normalized fluorescence (*F*) was plotted as a function of nominal [DEDIC], and the resulting quench curves were fitted to a two binding site model (eq. 26). Parameters obtained from replicate titrations (at least two) were averaged, yielding for *F1*S* (circles), $K^1_{D(F1*S)} = 0.041 \pm 0.010$ μM, $n^1{}_{(F1*S)} = 0.69 \pm 0.02$, $K^2_{D(F1*S)} = 29 \pm 7$ μM, and $n^2{}_{(F1*S)}$ was indeterminate. For the *A* variant (squares), $K^1_{D(A)} = 0.31 \pm 0.18$ μM, and $K^2_{D(A)} = 8.8 \pm 0.7$ μM, with both $n^1{}_{(A)}$ and $n^2{}_{(A)}$ indeterminate; and for whole AGP (triangles), $K^1_{D(native)} = 0.049 \pm 0.005$ μM, $n_1 = 0.63 \pm 0.04$ μM, and $K^2_{D(native)} = 12 \pm 2$ μM, with n_2 indeterminate. Note also that for both the isolated variants and whole AGP, the fraction of fluorescence unquenched at limiting nominal [DEDIC] is 0.21 ± 0.02.

The isolated protein variants *F1*S* and *A* were quenched similarly by DEDIC (Figure 6, circles and squares, respectively). Both data sets suggest the existence of two classes of binding sites, and neither could be fit satisfactorily to a one-site model. The data for the *F1*S* and *A* variants also were fitted by eq. 26, which assumes two sites per protein molecule. This treatment gave for the *F1*S* variant $K^1_{D(F1*S/DEDIC)} = 0.041 \pm 0.010$ μM with $n^1{}_{(F1*S)} = 0.69 \pm 0.02$ μM, and $K^2_{D(F1*S/DEDIC)} = 29 \pm 7$ μM with $n^2{}_{(F1*S)}$ indeterminate. The normalized amplitudes of the two processes were $A^1{}_{(F1*S)} = 0.62 \pm 0.03$ and $A^2{}_{(F1*S)} = 0.20 \pm 0.02$ with an unquenched fraction having $A^3{}_{(F1*S)} = 0.18 \pm 0.02$. For the *A* variant, $K^1_{D(A/DEDIC)} = 0.31 \pm 0.10$ μM and $K^2_{D(A/DEDIC)} = 8.8 \pm 0.7$ μM with both $n^1{}_{(A)}$ and $n^2{}_{(A)}$ indeterminate. The normalized amplitudes of the two processes were $A^1{}_{(A)} = 0.31 \pm 0.02$ and $A^2{}_{(A)} = 0.44 \pm 0.02$ with an unquenched fraction having $A_{unq} = 0.25 \pm 0.02$.

Note that in these experiments the *free* concentration of DEDIC is much smaller than the *nominal* concentration (given on the abscissa of Figure 6), because of high affinity binding. The K_D (e.g., 0.049 μM) is therefore well below the apparent high affinity IC_{50} (0.21 μM). (In general, for a one-site model, the K_D is smaller than the IC_{50} by an amount equal to one-half the nominal protein concentration.)

In summary, in whole AGP, DEDIC is selective both for the *F1*S* high affinity site over the *F1*S* low affinity site and for the *F1*S* high affinity site over the *A* high affinity site by factors of 700 and 8, respectively.

Proof of Method

Using DEDIC to Determine Inhibition Constants for Drug Binding to the Isolated Variants

AMI and BUP are members of a large class of ligands that produce no appreciable alteration in the fluorescence of a protein when they bind. Indeed, AMI and BUP were chosen to illustrate

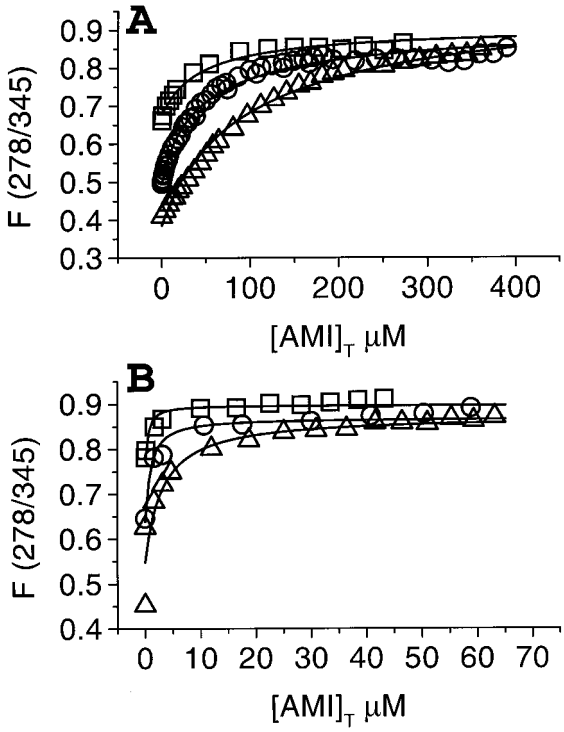

Figure 7. (**A**) Fluorescence recovery following addition of AMI to a pre-equilibrated solution of 0.39 μM *A* variant and 1 μM DEDIC (squares), 2.5 μM DEDIC (circles), or 10 μM DEDIC (triangles). All concentrations are nominal. The recovery curves were plotted simultaneously to a model of competitive inhibition (eq. 36) to yield $K_{I(A)}^{AMI} = 0.10 \pm 0.01$ μM. (**B**) Fluorescence recovery following addition of AMI to a pre-equilibrated solution of 0.39 μM *F1*S* variant and 0.2 μM DEDIC (squares), 0.4 μM DEDIC (circles), or 1 μM DEDIC (triangles). Fitting the data to eq. 36 gave $K_{I(F1*S)}^{AMI} = 4.6 \pm 0.3$ μM.

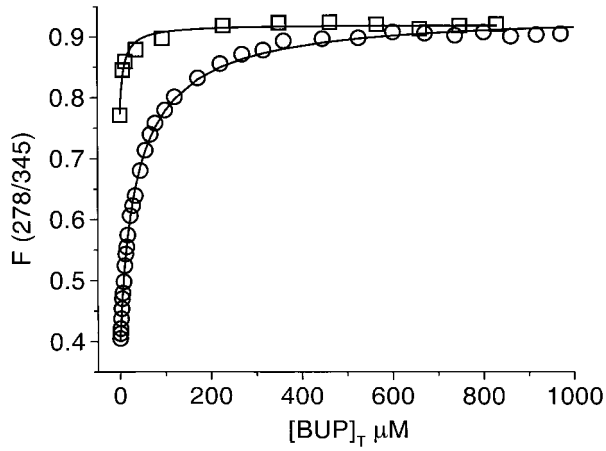

Figure 8. Addition of the nonquenching drug BUP to a mixture of 1 μM DEDIC (nominal) and 0.39 μM of the isolated variant results in fluorescence recovery. (Squares and circles represent the *A* and *F1*S* variants, respectively.) This recovery was successfully fitted to a model of competitive inhibition (eq. 36), yielding K_I(BUP/A) = 1.9 ± 0.4 μM and K_I(BUP/*F1*S*) = 1.7 ± 0.1 μM.

the utility of DEDIC in the spectrofluorometric determination of ligand affinity to the isolated variants.

The equilibrium fluorescence recovery that is reached following addition of AMI to DEDIC-quenched *A* and *F1*S* variants is shown in Figures 7A and 7B, respectively. Experiments were repeated several times at different nominal [DEDIC]. Using a model of competitive antagonism, eq. 36 (see Appendix) and the parameters already reported for DEDIC binding, K_I(AMI) for the *A* and *F1*S* variants were determined to be 0.10 ± 0.01 μM (*A*) and 4.6 ± 0.3 μM (*F1*S*).

For both variants, the simultaneous fit of the several curves by single values of K_I(AMI) was consistent with a model of competitive antagonism. Moreover, the measured inhibition constants were comparable to those determined by Hervé[1] using equilibrium dialysis: K_D(*A*/AMI) = 0.30 ± 0.02 μM and K_D(*F1*S*/AMI) = 13.5 ± 13.2 μM.

In competition with DEDIC, BUP also reversed the quenching of both variants, *A* and *F1*S* (Figure 8, squares and circles, respectively). This recovery was successfully fitted to a model of competitive inhibition, yielding K_I(BUP/A) = 1.9 ± 0.4 μM and K_I(BUP/F1*S) = 1.7 ± 0.1 μM. BUP therefore binds with equal affinity to both variants. Although the apparent affinity of BUP to native AGP has been reported (0.9 μM),[16] its affinity to the isolated variants has not. However, given that BUP binds to both with equal affinities, its apparent K_D for binding to whole AGP is ~2 μM, which is in near agreement with the previously reported K_D of 0.9 μM (standard error not reported), as determined by BUP competition experiments on a mixture of AGP using the fluorescent probe 8-ANS.

*Using DEDIC to Determine Drug Affinity for the F1*S Variant in Whole (Native) AGP*

The fluorescence recovery following addition of a competitor (AMI and BUP) to a pre-equilibrated mixture of 1 μM DEDIC and 0.39 μM native AGP

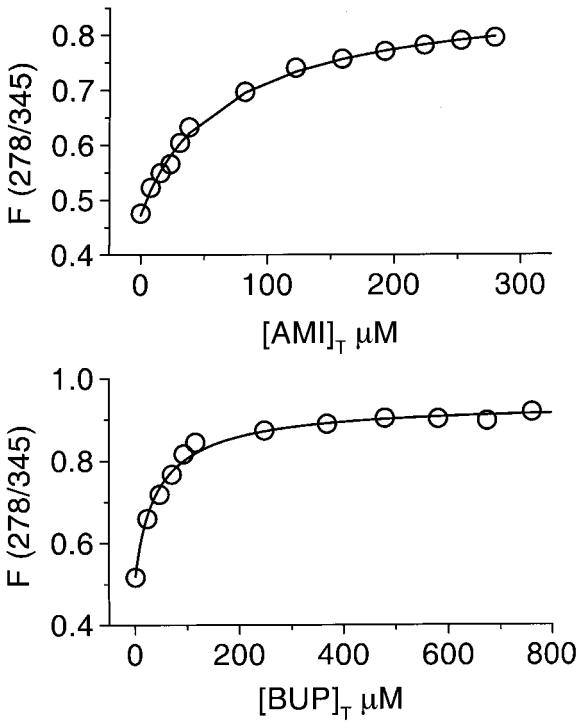

Figure 9. Drug inhibition constants for the *F1*S* variant were determined using DEDIC and whole (unfractionated) AGP. The addition of the nonquenching drugs BUP and AMI to a mixture of 1 μM DEDIC (nominal) and 0.39 μM native AGP resulted in fluorescence recovery. The curves were fitted to eq. 36 to yield inhibition constants for $K_{D(F1*S)}^{AMI}$ and $K_{D(F1*S)}^{BUP}$ of 3.0 ± 0.5 and 1.9 ± 0.1 μM, for AMI and BUP, respectively.

(nominal concentrations) is shown in Figure 9. Given the ~10-fold selectivity of DEDIC for binding to the high affinity site on the *F1*S* variant over both the sites on the *A* variant and the lower affinity site on *F1*S*, it was possible to select a nominal DEDIC concentration (1 μM with [AGP] = 0.39 μM) for which DEDIC occupied only high affinity *F1*S* sites. Therefore, in the competition experiment, one observes only the displacement of DEDIC from *F1*S*, regardless of whether or not the *A* variant is present in solution. In this manner, K_I(AMI/*F1*S*) was determined to be 3.0 ± 0.5 μM, which is in agreement with the K_I already determined with the isolated *F1*S* variant (i.e., 4.6 ± 0.3 μM). Likewise, K_I(BUP/*F1*S*) was determined to be 1.9 ± 0.1 μM, which is in agreement with that previously determined using the isolated *F1*S* variant (i.e., 1.7 ± 0.1 μM).

Potential of DEDIC as a More General Probe of Drug–Protein Interactions

Preliminary experiments in this lab have shown that DEDIC quenches the native tryptophan fluorescence of human serum albumin (HSA) in a concentration-dependent manner. Fitting the data (not shown) to a single-binding-site model gave a K_D of 3.3 ± 0.5 μM. We also observe that DEDIC interacts with chain *A* of the lipocalin bovine beta lactoglobulin (BLG-*A*), a structural homologue of AGP, to produce changes in fluorescence (data not shown). With BLG, however, the concentration dependence is biphasic. At low (substoichiometric) concentrations of DEDIC, the fluorescence is enhanced, but further elevation of [DEDIC] results in fluorescence quenching. Experiments are ongoing to investigate both the identity of the DEDIC binding sites on these proteins and to examine the displacement of DEDIC by added drugs.

DISCUSSION

Design and Synthesis of DEDIC

DEDIC was the product of an effort to characterize the binding of local anesthetics (LAs) to AGP. The LA BUP, for example, had been reported to be heavily (95%) bound to AGP in human serum.[17] However, we observed that many LAs (including BUP and lidocaine) produced little or no change in either the absorbance or fluorescence of AGP on addition.

Thus, we based the structure of DEDIC on that of an archetypal LA, having a hydrophobic aromatic moiety connected to a relatively hydrophilic tertiary amine via a polar (ester or amide) linker. For DEDIC, an amide bond was selected because of its greater resistance both to hydrolysis and degradation by adventitious pseudoacetylcholinesterases in biological samples. To produce a likely quencher, we chose to append two iodine atoms to the hydrophobic ring. Specifically, a salicylate moiety was chosen because of its directing effects during iodination, although the final synthesis of DEDIC was achieved without having to perform the iodination.

Although it is plausible that the appended iodines of DEDIC are indeed responsible for its quenching of AGP, it is equally plausible that quenching occurs via fluorescence resonance energy transfer between an excited tryptophyl donor (λ_{max}(em) = 340 nm and DEDIC

(λ_{max}(abs) = 355 nm). Significantly, two molecules that do not quench protein fluorescence on binding to high affinity sites, BUP and AMI, are nonabsorbing at wavelengths > 280 and 300 nm, respectively. Moreover, the drug DIP is a quencher; although lacking iodines, it absorbs in the region of maximum AGP fluorescence, with separate peaks centered near 280 and 420 nm. We did not attempt to differentiate between these mechanisms in this report.

Finally, a DED moiety (as occurs on the LA procainamide) was employed as a hydrophilic head after an attempt with the less hydrophilic dibutyl analog resulted in a probe having a solubility too low to be useful.

The synthesis of DEDIC as described herein was convenient for making large quantities of the compound from readily available, inexpensive materials. Our previous attempts had involved iodinating 2-hydroxy-*N*-[2(diethylamino)ethyl]-benzamide, but this procedure yielded a mixture of mono- and diiodinated products that were difficult to isolate on a preparative scale. The success of the current method is particularly dependent on the specific conditions described because they minimized polymerization of the diiodosalicyl chloride intermediate and also efficiently removed principal contaminants from the product.

Noteworthy Physical Properties

With pK_as of 5.0 and 9.8, DEDIC is a zwitterion at physiologic pH (7.4). The acidity of the phenolic hydrogen of DEDIC was initially surprising, but may be explained, in part, by the inductive effects of the ortho and para iodines. Additionally, if zwitterionic DEDIC can participate in either intra- or intermolecular hydrogen bonding, then this bonding would also act to lower the observed pK_a^1. In agreement with these hypothetical interactions, it has been reported that the structurally analogous drug raclopride,[18] a 3,5-dichlorosalicylamide, has a pK_a^1 near 4 and pK_a^2 near 9.5.

Separation of AGP Into the Major Variants *A* and *F1*S*

The chromatographically separated variants *A* and *F1*S* possessed absorbance and fluorescence spectra of the same shape as that of whole AGP. Their relative abundances (81% *F1*S* and 19% *A*) were similar to those reported by Halsall[15] (75 and 25%, respectively).

Confirming our assignment of chromatographic fractions to the AGP variants, the affinity of the *A* and *F1*S* variants for DIP (0.75 ± 0.12 and 0.07 ± 0.02 μM, respectively) agree to within a factor of three with those previously reported by Hervé[7] using equilibrium dialysis: 2.9 ± 0.04 and 0.31 ± 0.02 μM, respectively. Moreover, our ratio of the affinities of DIP for the *F1*S* and *A* variants (10.7) is comparable to Hervé's (9.4). The small (factor of three) differences between the absolute affinities are not unexpected given the differences in both the ionic strength and composition of the buffer. Furthermore, we noted that DIP could form supersaturated solutions, which decayed to their equilibrium solubilities over a period of hours to days. Hervé reported using concentrations of DIP in her buffer solutions that were up to 10-fold more concentrated than we could achieve in ours, which also might account for the small discrepancy.

Utility of DEDIC as a Probe of Interactions Between Drugs and Isolated AGP Variants

Addition to a pre-equilibrated solution of AGP and DEDIC of a drug that minimally (0–10%) quenches, such as BUP or AMI, results in fluorescence recovery from which the equilibrium inhibition constants can be calculated without radiolabelling or drug modifications of any kind. Equilibrium interactions are achieved within a few seconds, and one sample of protein can be examined with increasing concentrations of the drug in question.

For both variants, the simultaneous fit of the several curves by single values of K_I(AMI) was consistent with a model of competitive antagonism. Moreover, the measured inhibition constants, 0.10 ± 0.01 μM (*A*) and 4.6 ± 0.3 μM (*F1*S*), were comparable to those determined by Hervé[1] using equilibrium dialysis: K_D(*A*/AMI) = 0.30 ± 0.02 μM and K_D(*F1*S*/AMI) = 13.5 ± 13.2 μM. As was observed with DIP, the calculated inhibition constants for AMI were each roughly three-fold lower than those previously determined using equilibrium dialysis.[1] As with DIP, our calculated selectivity of AMI for the *F1S* variant (46 ± 5) agrees with that reported by Hervé (i.e., 45 ± 44).

Of further interest here is the finding that BUP binds to the two variants with comparable affinities. Whereas a K_D for BUP binding to whole AGP has been previously reported (0.9 μM[16]), these are the first reports of the affinities of BUP

for the individual variants. As reported by Hervé,[1] the structurally and functionally related compound lidocaine also displays little variant selectivity.

*Utility of DEDIC as a Probe of Drug Interactions With the F1*S Variant in Whole (Native) AGP*

Because DEDIC binds selectively to the high affinity site on the *F1*S* variant, it can be used to probe the association of drugs to *F1*S* when both variants are present, as in whole AGP. The agreement between the inhibition constants calculated for AMI and BUP, K_{Is} (*F1*S*), obtained in whole AGP and those obtained in the isolated variant confirms the utility of DEDIC as a probe of binding to the *F1*S* variant in the naturally occurring mixture. Moreover, the use of the strongly *A* variant-selective drug AMI provided a particularly stringent test of the ability of DEDIC to selectively probe binding to the *F1*S* variant in native AGP. In short, DEDIC offers a convenient method for the accurate determination of ligand affinities without the need to first separate the variants.

Comparing DEDIC With Other Probes of Drug–AGP Binding

Spectrofluorometric measurements of drug–protein binding may be of two types; they are, *direct* and *indirect*. Direct spectrofluorometric determination of drug affinities requires that either the drug or the protein exhibit binding-dependent changes in fluorescence. Clearly, this requirement constrains the utility of the method because the binding of many drugs produces no detectable changes in optical signals; that is, a drug may not possess an appreciable fluorescence or, if it does, the spectrum is not altered by protein binding. Notwithstanding, this method has been applied to examine the binding of both nonfluorescent, quenching drugs (e.g., DIP and CPZ[19]) and fluorescent drugs whose intensity increases on binding (e.g., warfarin[20]). We used this approach in our direct determination of the K_D for DIP binding to the *F1*S* variant, 0.13 ± 0.03 μM, which approximates the previously reported value of 0.38 ± 0.01 μM as determined by equilibrium dialysis in 0.067 M phosphate buffer at pH 7.40.[1]

In cases where the direct observation of binding is not possible, indirect methods have been used. Traditionally, these rely on antagonism between the drug and a fluorescent probe whereby the displacement of probe by the drug is observed as a decrease in the fluorescence of the probe. Then, given the affinity of the probe for AGP, the affinity of the drug may be calculated. The probes ANS[21,22,23] and auramine O are commonly used for this purpose.

Here, however, we report the use of the complementary method: the use of a reversibly bound probe (DEDIC) as a quencher of the intrinsic fluorescence of AGP. Although the drugs CPZ and DIP have been reported to quench AGP,[19] they have not been used as spectrofluorometric probes of drug binding. Even so, DEDIC would possess a significant advantage over them in terms of its ability to probe variant-specific binding. CPZ does not exhibit variant-selective binding as indicated by its almost equal affinities to bind the *F1*S* and *A* variants (0.37 ± 0.03 and 0.74 ± 0.09,[7] respectively). Furthermore, DEDIC is a more versatile probe than DIP. Indeed, while possessing a selectivity for the *F1*S* variant comparable to that of DIP, DEDIC not only binds *F1*S* with almost a 10-fold higher affinity (0.041 ± 0.010 μM) than does DIP (0.31 ± 0.02 μM[7]), but also has 40-fold greater solubility, a property that permits its additional use as a general probe of drug binding to lower affinity sites on either variant.

For drugs that produce a relatively small fluorescence change (e.g., $< 20\%$), DEDIC provides a means of amplifying the signal change that occurs on binding because limiting concentrations of DEDIC quench roughly 80% of the native protein fluorescence. In addition, because DEDIC binds selectively to the *F1*S* variant of AGP, the *F1*S* affinities of partial quenchers may be determined in a mixture of variants, such as occurs naturally in AGP, thereby eliminating the need to separate them chromatographically. For example, limiting concentrations of the tricyclic antidepressant AMI quench ~8% of the fluorescence of AGP (data not shown), but this small signal change did not permit us to directly determine its precise affinity. Using DEDIC as a probe of AMI binding, however, we were able to determine affinities of the drug for both variants. In addition, DEDIC allowed us to determine the *F1*S* affinity of this strongly *A* variant-selective drug in native AGP.

Our work suggests that the binding of many drugs produces little, if any, change in protein fluorescence. Indeed, only minimal (0–8%) quenching of the fluorescence of AGP is produced by

representative drugs from three major classes: the local anesthetic BUP, the steroid progesterone, and the tricyclic antidepressant AMI.

For drugs producing larger fluorescence changes (e.g., $>20\%$) on binding, it is obviously not necessary to use a probe such as DEDIC to obtain a suitably large signal. Even with these quenching drugs, however, DEDIC could still be useful as a probe of drug binding to the F1*S variant in native AGP.

Interest in AGP has been growing amid reports that it may play a role in mediating inflammation,[24,25] so we hope that the methods presented here will prove useful in studying drug–AGP binding and perhaps contribute to our knowledge of the structure and function of this important protein.

NOMENCLATURE

DEDIC	2-hydroxy-3,5-diiodo-N[2(diethylamino)ethyl] benzamide
AGP	alpha 1-acid glycoprotein
HSA	human serum albumin
BLG-*A*	bovine beta lactoglobulin, Chain *A*
IMI	imipramine
DIP	dipyridamole
BUP	bupivacaine
8-ANS	8-anilinonaphthalenesulfonic acid
AMI	amitriptyline
*F1*S*	*F1* and *S* variants of AGP
AGP-A	gene encoding for the *F1* and *S* variants of AGP
AGP-B/*B'*	gene encoding for the *A* variant of AGP
DED	*N,N*-diethylethylenediamine
DIS	3,5-diiodosalicylic acid
SAM	standard aqueous medium, containing 0.15 M NaCl and 5 mM MOPS buffer adjusted to pH 7.40
F_{raw}	raw fluorescence
F	fluorescence corrected for inner filter and Raman errors and then normalized to unity
$F(\lambda_{ex}/\lambda_{em})$	corrected, normalized fluorescence with excitation and emission at λ_{ex} and λ_{em}
F_{rel}	quotient of the corrected, normalized fluorescence emission spectrum in the presence of a quencher divided by that obtained in its absence
n	ratio of binding site concentration to nominal protein concentration

ACKNOWLEDGMENTS

This research was supported in part by NIH grant GM35647 (to GRS) and a graduate stipend to LPC from the BWH Anesthesia Foundation.

APPENDIX

Derivation of the One-Site Binding Isotherm

The drug D is assumed to bind reversibly to the protein P to form a complex DP with an equilibrium dissociation constant of K_D. The nominal [D] and [P] are denoted D_T and P_T, respectively, and the fluorescence of P and DP is given by the product of their concentrations with their molar emissivity f. No fluorescence arises from free drug.

From the equilibrium condition and mass conservation we obtain the following:

$$K_D = \frac{[D][P]}{[DP]} \tag{1}$$

$$D_T = [D] + [DP] \tag{2}$$

$$P_T = [P] + [DP] \tag{3}$$

From eqs. 2 and 3, it follows that

$$[DP] = D_T - [D] \tag{4}$$

$$[P] = [P_T] - [DP] = P_T - (D_T - [D]) \tag{5}$$

Substituting eqs. 4 and 5 into eq. 1 and rearranging yields a quadratic equation:

$$[D]^2 + [D](P_T - D_T + K_D) - K_D D_T = 0 \tag{6}$$

for which the only physically meaningful root is

$$[D] = \frac{1}{2}\left(D_T - P_T r - K_D + \sqrt{K_D^2 + 2K_D P_T + 2K_D D_T + P_T^2 - 2D_T P_T + D_T^2}\right) \tag{7}$$

Neglecting the effects of dynamic quenching (which we already argued to be negligible), the observed fluorescence (corrected for inner-filter effects and background; e.g., Raman scatter from water) is given by

$$F = f_P[P] + f_{DP}[DP] \tag{8}$$

because the molar fluorescence of the drug is zero.

Substituting eqs. 4 and 5 into eq. 8 yields

$$F = f_{\mathrm{P}}\left[\frac{K_{\mathrm{D}}}{K_{\mathrm{D}} + [\mathrm{D}]}\right]P_{\mathrm{T}} + f_{\mathrm{DP}}\left[\frac{[\mathrm{D}]}{K_{\mathrm{D}} + [\mathrm{D}]}\right]P_{\mathrm{T}} \qquad (9)$$

where [D] is given by eq. 7.

If the fluorescence data are normalized to unity from drug–free protein, then

$$F \equiv 1 = f_{\mathrm{P}}P_{\mathrm{T}} \qquad (10)$$

Using eqs. 3 and 10, substituting into eq. 8, and rearranging yields

$$F = 1 - (f_{\mathrm{P}} - f_{\mathrm{DP}})P_{\mathrm{T}} + [\mathrm{DP}] \qquad (11)$$

Defining the amplitude A of the change due to drug-induced quenching as follows:

$$A \equiv (f_{\mathrm{P}} - f_{\mathrm{DP}})P_{\mathrm{T}} \qquad (12)$$

and substituting eq. 4 into eq. 11 and rearranging gives

$$F = 1 - A\left[\frac{[\mathrm{D}]}{[\mathrm{D}] + K_{\mathrm{D}}}\right] \qquad (13)$$

where [D] is not identical to the nominal drug concentration, but is again given by eq. 7.

Derivation Of the Two-Site Binding Isotherm

The drug D is assumed to bind reversibly to two noninteracting sites, P_1 and P_2, to form complexes DP_1 and DP_2, with respective equilibrium dissociation constants K_{D}^1 and K_{D}^2. The nominal concentrations of the sites are denoted P_1^{T} and P_2^{T}. The species P_1, P_2, DP_1, and DP_2 each contributes to the measured fluorescence F by an amount equal to the product of their concentrations and their respective molar fluorescences, f. No fluorescence arises from the drug.

From equilibrium and mass conservation, we get

$$\begin{aligned} K_{\mathrm{D}}^1 &= \frac{[\mathrm{D}][\mathrm{P}_1]}{[\mathrm{DP}_1]} \\ K_{\mathrm{D}}^2 &= \frac{[\mathrm{D}][\mathrm{P}_2]}{[\mathrm{DP}_2]} \end{aligned} \qquad (14)$$

$$\begin{aligned} P_1^{\mathrm{T}} &= [\mathrm{P}_1] + [\mathrm{DP}_1] \\ P_2^{\mathrm{T}} &= [\mathrm{P}_2] + [\mathrm{DP}_2] \end{aligned} \qquad (15)$$

$$\begin{aligned} [\mathrm{P}_1] &= P_1^{\mathrm{T}} - [\mathrm{DP}] = P_1^{\mathrm{T}} - (D_{\mathrm{T}} - [\mathrm{D}]) \\ [\mathrm{P}_2] &= P_2^{\mathrm{T}} - [\mathrm{DP}] = P_2^{\mathrm{T}} - (D_{\mathrm{T}} - [\mathrm{D}]) \end{aligned} \qquad (16)$$

Substituting eqs. 16 into eqs. 14 and solving for [DP] yield the familiar relations

$$\begin{aligned} [\mathrm{DP}_1] &= \left[\frac{[\mathrm{D}]}{K_{\mathrm{D}}^1 + [\mathrm{D}]}\right]P_1^{\mathrm{T}} \\ [\mathrm{DP}_2] &= \left[\frac{[\mathrm{D}]}{K_{\mathrm{D}}^2 + [\mathrm{D}]}\right]P_2^{\mathrm{T}} \end{aligned} \qquad (17)$$

Now, from mass conservation of drug

$$D = D_{\mathrm{T}} - [\mathrm{DP}]_1 - [\mathrm{DP}_2] \qquad (18)$$

and substituting eqs. 17, the following relationship is formed:

$$D = D_{\mathrm{T}} - \left[\frac{[\mathrm{D}]}{K_{\mathrm{D}}^1 + [\mathrm{D}]}\right]P_1^{\mathrm{T}} - \left[\frac{[\mathrm{D}]}{K_{\mathrm{D}}^2 + [\mathrm{D}]}\right]P_2^{\mathrm{T}} \qquad (19)$$

Equation 19 is a cubic equation that may be solved[27] for [D]:

$$[\mathrm{D}](D_{\mathrm{T}}, P_1^{\mathrm{T}}, P_2^{\mathrm{T}}, K_{\mathrm{D}}^1, K_{\mathrm{D}}^2) = -\frac{a}{3} + \frac{2}{3}\sqrt{a^2 - 3b}\cdot\cos\frac{\theta}{3} \qquad (20)$$

where

$$\begin{aligned} a &= K_{\mathrm{D}}^1 + K_{\mathrm{D}}^2 + P_{\mathrm{T}}^1 + P_{\mathrm{T}}^2 + D_{\mathrm{T}} \\ b &= K_{\mathrm{D}}^1\,K_{\mathrm{D}}^2 + P_1^{\mathrm{T}}\,(K_{\mathrm{D}}^2 - K_{\mathrm{D}}^1) - D_{\mathrm{T}}\,(K_{\mathrm{D}}^1 + K_{\mathrm{D}}^2) \\ c &= -K_{\mathrm{D}}^1\,K_{\mathrm{D}}^2\,D_{\mathrm{T}} \\ \theta &= \arccos\left[\frac{-2\mathrm{a}^3 + 9\mathrm{ab} - 27\mathrm{c}}{2\sqrt{(\mathrm{a}^2 - 3\mathrm{b})^3}}\right] \end{aligned}$$

Substitution of eq. 20 into eqs. 16 and 17 gives expressions for the equilibrium values of the species $[\mathrm{P}_1]$, $[\mathrm{P}_2]$, $[\mathrm{DP}_1]$, and $[\mathrm{DP}_2]$.

The observed fluorescence is given by

$$F = f_{\mathrm{P}_1}[\mathrm{P}_1] + f_{\mathrm{P}_2}[\mathrm{P}_2] + f_{\mathrm{DP}_1}[\mathrm{DP}]_1 + f_{\mathrm{DP}_2}[\mathrm{DP}_2] \qquad (21)$$

Substituting eqs. 16 and 17 into eq. 21 gives

$$\begin{aligned} F = {} & f_{\mathrm{P}_1}\left[\frac{K_{\mathrm{D}}^1}{K_{\mathrm{D}}^1 + [\mathrm{D}]}\right]P_1^{\mathrm{T}} + f_{\mathrm{P}_2}\left[\frac{K_{\mathrm{D}}^2}{K_{\mathrm{D}}^2 + [\mathrm{D}]}\right]P_2^{\mathrm{T}} \\ & + f_{\mathrm{DP}_1}\left[\frac{[\mathrm{D}]}{K_{\mathrm{D}}^1 + [\mathrm{D}]}\right]P_1^{\mathrm{T}} + f_{\mathrm{DP}_2}\left[\frac{[\mathrm{D}]}{K_{\mathrm{D}}^2 + [\mathrm{D}]}\right]P_2^{\mathrm{T}} \end{aligned} \qquad (22)$$

which rearranges to

$$F = \left[\frac{f_{P_1}K_D^1 + f_{DP_1}[D]}{K_D^1 + [D]}\right]P_1^T + \left[\frac{f_{P_2}K_D^2 + f_{DP_2}[D]}{K_D^2 + [D]}\right]P_2^T \tag{23}$$

In addition, if the data are normalized, then

$$F \equiv 1 = f_{P_1}P_1^T + f_{P_2}P_2^T \tag{24}$$

Substituting into eq. 21 making use of eqs. 15 and 24 gives

$$F = 1 - (f_{P_1} - f_{DP_1})P_1^T - (f_{P_2} - f_{DP_2})P_2^T \tag{25}$$

Finally, substituting for DP_1 and DP_2 using eqs. 17 gives

$$F = 1 - A_1\left[\frac{[D]}{K_D^1 + [D]}\right] - A_2\left[\frac{[D]}{K_D^2 + [D]}\right] \tag{26}$$

where the amplitudes A_1 and A_2 are defined as

$$\begin{aligned} A_1 &\equiv (f_{P_1} - f_{DP_1})P_1^T \\ A_2 &\equiv (f_{P_2} - f_{DP_2})P_2^T \end{aligned} \tag{27}$$

Equations 23 and 27 are also applicable to the case of both independent protein binding sites being on the same molecule.

Derivation of the One-Site Competition Equation

The situation here (two drugs D_1 and D_2 competing for a single site on the protein) is mathematically analogous to that of two proteins competing for a single drug, which has been described in detail in the last section. Thus by transposing the "drug" and "protein" terms in eq. 20, one obtains an expression for the concentration of [P] as a function of the total drug concentrations.

$$[P](P_T, D_1^T, D_2^T, K_D^1, K_D^2) = -\frac{a}{3} + \frac{2}{3}\sqrt{a^2 - 3b}\cdot\cos\frac{\theta}{3} \tag{28}$$

where

$$\begin{aligned} a &= K_D^1 + K_D^2 + D_T^1 + D_T^2 + P_T, \\ b &= K_D^1K_D^2 + D_1^T(K_D^2 - K_D^1) - P_T(K_D^1 + K_D^2), \\ c &= -K_D^1K_D^2P_T, \end{aligned}$$

and

$$\theta = \arccos\left[\frac{-2a^3 + 9ab - 27c}{2\sqrt{(a^2 - 3b)^3}}\right].$$

The observed fluorescence is given by

$$F = f_P[P] + f_{PD_1}[PD_1] + f_{PD_2}[PD_2] \tag{29}$$

By mass conservation of protein,

$$P = P_T - [PD_1] - [PD_2] \tag{30}$$

Substituting eq. 30 into eq. 29 and rearranging yields the analog of eq. 25:

$$F = f_PP^T - (f_P - f_{PD_1})D_1^T - (f_P - f_{PD_2})D_2^T \tag{31}$$

Substituting the analogs of eq. 17

$$\begin{aligned} [PD_1] &= \left[\frac{[P]}{K_D^1 + [P]}\right]D_1^T \\ [PD_2] &= \left[\frac{[P]}{K_D^2 + [P]}\right]D_2^T \end{aligned} \tag{32}$$

gives

$$F = f_PP^T - A_1\cdot\left[\frac{[P]}{K_D^1 + [P]}\right] - A_2\cdot\left[\frac{[P]}{K_D^2 + [P]}\right] \tag{33}$$

where the amplitudes A_1 and A_2 are defined as

$$\begin{aligned} A_1 &\equiv (f_P - f_{PD_1})D_1^T \\ A_2 &\equiv (f_P - f_{PD_2})D_2^T \end{aligned} \tag{34}$$

If the data are normalized to unity, then

$$F \equiv 1 = f_P\cdot P^T \tag{35}$$

and

$$F = 1 - A_1\left[\frac{[P]}{K_D^1 + [P]}\right] - A_2\left[\frac{[P]}{K_D^2 + [P]}\right] \tag{36}$$

REFERENCES

1. Hervé F, Caron G, Duche JC, Gaillard P, Abd RN, Tsantili-Kakoulidou A, Carrupt PA, d'Athis P, Tillement JP, Testa B. 1998. Ligand specificity of the genetic variants of human alpha1-acid glycoprotein: generation of a three-dimensional quantitative structure-activity relationship model for drug binding to the A variant. Mol Pharmacol 54:129–138.
2. Kremer JM, Wilting J, Janssen LH. 1988. Drug binding to human alpha-1-acid glycoprotein in health and disease. Pharmacol Rev 40:1–47.

3. Routledge PA. 1986. The plasma protein binding of basic drugs. Br J Clin Pharmacol 22:499–506.
4. Eap CB, Baumann P. 1989. The genetic polymorphism of human alpha 1-acid glycoprotein. Prog Clin Biol Res 300:111–125.
5. Hervé F, Duche JC, Barre J, Millot MC, Tillement JP. 1992. pH titration curves of the desialylated human alpha 1-acid glycoprotein variants by combined isoelectrofocusing-electrophoresis: Utilization in the development of a fractionation method for the protein variants by chromatography on immobilized metal affinity adsorbent. J Chromatogr 577:43–59.
6. Hervé F, Gomas E, Duche JC, Tillement JP. 1993. Evidence for differences in the binding of drugs to the two main genetic variants of human alpha 1-acid glycoprotein. Br J Clin Pharmacol 36:241–249.
7. Hervé F, Duche JC, d'Athis P, Marche C, Barre J, Tillement JP. 1996. Binding of disopyramide, methadone, dipyridamole, chlorpromazine, lignocaine and progesterone to the two main genetic variants of human alpha 1-acid glycoprotein: Evidence for drug-binding differences between the variants and for the presence of two separate drug-binding sites on alpha 1-acid glycoprotein. Pharmacogenetics 6:403–415.
8. Dente L, Pizza MG, Metspalu A, Cortese R. 1987. Structure and expression of the genes coding for human alpha 1-acid glycoprotein. EMBO J 6:2289–2296.
9. Tomei L, Eap CB, Baumann P, Dente L. 1989. Use of transgenic mice for the characterization of human alpha 1-acid glycoprotein (orosomucoid) variants. Hum Genet 84:89–91.
10. Hervé F, Gomas E, Duche JC, Tillement JP. 1993. Fractionation of the genetic variants of human alpha 1-acid glycoprotein in the native form by chromatography on an immobilized copper(II) affinity adsorbent. Heterogeneity of the separate variants by isoelectrofocusing and by concanavalin A affinity chromatography. J Chromatogr 615:47–57.
11. Sun H, Dage JL, Halsall HB. 1996. Separation of human orosomucoid major gene products using immobilized copper affinity chromatography and identification of the metal-interactive residues. Chromatographia 46:430–436.
12. Oravcova J, Bohs B, Lindner W. 1996. Drug-protein binding sites. New trends in analytical and experimental methodology. J Chromatogr B Biomed Appl 677:1–28.
13. Lakowicz JR. 1999. In Principles of Fluorescence Spectroscopy, 2nd Edition. New York: Kluwer Academic/Plenum Publishers.
14. Hof M, Vajda S, Fidler V, Karpenko V. 1996. Picosecond Tryptophan Fluorescence of Human Blood Serum Orosomucoid. Collect Czech Chem Commun 61:808–818.
15. Sun H. (H. Brian Halsall, Advisor) Characterization of the ligand-binding properties of human orosomucoid gene products I and Ii (lysine, histidine, warfarin, propranolol). Thesis, University Of Cincinnati. Cincinnati, OH; pp. 1–214.
16. Essassi D, Zini R, Tillement JP. 1989. ANS-drug interactions to AAG and HSA fluorescence and equilibrium dialysis studies. Prog Clin Biol Res 300:423–426.
17. Tucker GT, Mather LE. 1975. Pharmacology of local anaesthetic agents. Pharmacokinetics of local anaesthetic agents. Br J Anaesth 47: suppl.213–224.
18. Pagliara A, Carrupt PA, Caron G, Gaillard P, Testa B. 1997. Lipophilicity profiles of ampholytes. Chem.Rev (Washington, D.C.) 97:3385–3400.
19. Carrupt PA, Tsai RS, El Tayar N, Testa B, De Paulis T, Hoegberg T. 1991. Ionization behavior and ionization-dependent conformation of raclopride, a dopamine D2 receptor antagonist. Helv Chim Acta 74:956–968.
20. Friedman ML, Schlueter KT, Kirley TL, Halsall HB. 1985. Fluorescence quenching of human orosomucoid. Accessibility to drugs and small quenching agents. Biochem J 232:863–867.
21. Zini R, Copigneaux C, Tillement JP. 1989. 1-Anilino-naphthalene 8-sulfonic acid (ANS) as a probe for the binding of antidepressant drugs to human alpha 1-acid glycoprotein (AAG). Prog Clin Biol Res 300:417–421.
22. Epps DE, Raub TJ, Kezdy FJ. 1995. A general, wide-rage spectrofluorometric method for measuring the site- specific affinities of drugs toward human serum albumin. Anal Biochem 227:342–350.
23. Maruyama T, Furuie MA, Hibino S, Otagiri M. 1992. Comparative study of interaction mode of diazepines with human serum albumin and alpha 1-acid glycoprotein. J Pharm Sci 81:16–20.
24. Johansen AK, Willassen NP, Sager G. 1992. Fluorescence studies of beta-adrenergic ligand binding to alpha 1-acid glycoprotein with 1-anilino-8-naphthalene sulfonate, isoprenaline, adrenaline and propranolol. Biochem Pharmacol 43:725–729.
25. van Dijk W, Brinkman-van der Linden EC, Havenaar EC. 1998. Occurrence and possible function of inflammation-induced expression of sialyl Lewis-x on acute-phase proteins. Adv Exp Med Biol 435:145–150.
26. Shiyan SD, Bovin NV. 1997. Carbohydrate composition and immunomodulatory activity of different glycoforms of alpha1-acid glycoprotein. Glycoconj J 14:631–638.
27. Wang ZX, Jiang RF. 1996. A novel two-site binding equation presented in terms of the total ligand concentration. FEBS Lett 392:245–249.